

Optimal Management of Renewable Generation and Uncertain Demand with Reverse Fuel Cells by Stochastic Model Predictive Control

F. Conte

Campus Bio-Medico University of Rome
Faculty of Engineering
Via Alvaro del Portillo, 21
I-00128, Roma, Italy
f.conte@unicampus.it

G. Mosaico, G. Natrella, M. Saviozzi

University of Genoa
DITEN
Via all'Opera Pia 11 A
I-16145, Genova, Italy
matteo.saviozzi@unige.it

F. R. Bianchi

University of Genoa
DICCA
Via Montallegro 1
I-16100, Genova, Italy
fiammettarita.bianchi@edu.unige.it

Abstract—This paper proposes a control strategy for a Reverse Fuel Cell used to manage a Renewable Energy Community. A two-stage scenario-based Model Predictive Control algorithm is designed to define the best economic strategy to be followed during operation. Renewable energy generation and users' demand are forecasted by a suitably defined Discrete Markov Chain based method. The control algorithm is able to take into account the uncertainties of forecasts and the nonlinear behaviour of the Reversible Fuel Cell. The performance of proposed approach is tested on a Renewable Energy Community composed by an aggregation of industrial buildings equipped with PV.

Index Terms—Fuel Cells, Hydrogen, Stochastic Model Predictive Control, Renewable Energy Communities.

I. INTRODUCTION

During last years, the wide spread of Renewable Energy Sources (RESs) has led academic and industrial research to investigate methodologies and technologies which allow a better use of renewable generation to supply energy systems. In literature, different techniques have been studied to manage RES generation and to optimize the functioning. RESs, such as wind and solar, are variable and hard to predict, therefore many stochastic algorithms have been developed to optimally manage the uncertainties in their forecasts.

The integration of Energy Storage Systems (ESSs) is necessary to deal with RES forecasting errors and uncertainties in power demand, and to obtain power system flexibility, namely the ability of the system generators to react to unexpected changes in load or system component performance [1]. Electrochemical ESSs, such as, batteries, have been widely studied and many works on batteries management can be found in literature [2]. A valid and environmental-friendly alternative to batteries are Power to Hydrogen (P2H) systems in which possible generation surplus is transformed into hydrogen by an

This work was carried out in the framework of the grant PRIN-2017K4JZEE “Planning and flexible operation of micro-grids with generation, storage and demand control as a support to sustainable and efficient electrical power systems: regulatory aspects, modelling and experimental validation” financed by the Italian Ministry for Education, University and Research.

Electrolyzer (Ely) and stored in a tank [3]. The same hydrogen can be eventually converted back into electrical power by a Fuel Cell (FC) when power demand exceeds power generation. Depending on the technology, the Ely and the FC can be two different devices or a single reversible unit, called as Reverse Fuel Cell (RFC), working in FC or Ely mode alternatively [4].

RFC dynamic behaviour is more complex than the one of batteries. Its efficiency depends on the working point according to a nonlinear law and the switching between the two modes cannot be executed close to instantaneously as for batteries, but a transition step has to be considered. In this framework, the objective of this study is to develop an optimal control algorithm able to take into account the uncertainties of RES generation and users demand. In order to satisfy this requirement, we provide a detailed local model for RFC operation efficiency and a Discrete Markov Chain (DMC)-based forecast algorithm [5] for both load and renewable production. Moreover, we use a two-stage scenario-based programming approach [6], [7] to deal with nonlinearities and forecast uncertainties. The result is a stochastic Model Predictive Control (MPC) algorithm which optimizes the economic operation of a Renewable Energy Community (REC). The integration of these different approaches and technologies in the REC framework is not so common in previous works, which focused on an effective formulation of control system algorithms, not using a RFC detailed model, or on RFC behaviour without optimizing global operation [8], [9]

A REC is a legal entity introduced by the European Commission (EC) through the Clean energy for all Europeans package. In particular, the EC issued two directives IEM [10] and RED II [11] aiming at improving the uptake of energy communities, at making easier for citizens to integrate efficiently in the electricity system as active participants, and at strengthening the role of RES self-consumers and REC.

In this paper, we consider as case study a REC composed of a Photovoltaic (PV) power plant, a RFC unit based on Solid-Oxide Cell (SOC) technology to cope with uncertainties in

arXiv:2208.14163v1 [math.OC] 30 Aug 2022

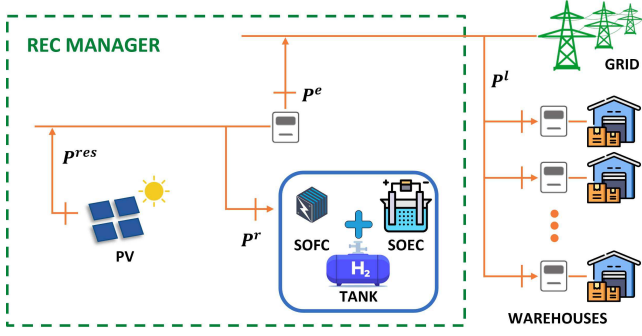


Figure 1. System Architecture.

the RES generation and power demand, and an aggregation of industrial warehouses operating as consumers. The manager of the REC administrate both RES generation and RFC operation, according to Italian transposition of European directives IEM and RED II.

The paper is organized as follows: section II introduces the system model, section III provides the control strategy, the case study is described in section IV, section V reports simulation results and the conclusions are reported in section VI.

II. SYSTEM MODEL

The schematic architecture of the considered system is reported in Figure 1. The REC is composed of a PV power plant and a RFC serving an aggregation of industrial warehouses. According to EU directives, the REC can supply the consumers' power demand and also export power to the grid. The industrial aggregation absorbs power from the PV plant and eventually from the grid, when the RES generation does not meet its demand. In the following, the models adopted for each system component are provided. In all, t indicates the discrete-time with a sampling time $\Delta=15$ min and reported powers are considered as mean values within the sampling interval.

A. Connection with the Main Grid

During the quarter hour t , the manager of the REC can export power P_t^e to the main grid. Therefore, it results that

$$0 \leq P_t^e \leq P_{max}^e, \quad (1)$$

where P_{max}^e is the maximum power exportable from REC.

B. RFC

The RFC absorbs power P_t^{el} to feed a tank with hydrogen as Solid-Oxide Electrolyzer Cell (SOEC) or generates power P_t^f by consuming stored hydrogen as Solid-Oxide Fuel Cell (SOFC). SOCs usually work at low pressures and high temperatures reducing crack formation probability and allowing high efficiencies. On the other hand a long start-up is required to reach requested operative temperatures with a time range depending on system size. SOEC and SOFC have different nonlinear efficiencies. Furthermore when switching from a mode of functioning to the other, the RFC does not produce nor consume hydrogen, but it demands power to maintain

constant its temperature. We indicate with \tilde{P}^{el} , the power supplied to the RFC when switching from SOFC to SOEC, and with \tilde{P}^f , the power supplied to the RFC, when switching from SOEC to SOFC. Due to slow thermal response, in this application we have decided to set the RFC always on. Equations describing the RFC functioning and hydrogen tank managing are reported below:

$$P_t^r = P_t^{el} \delta_t^{el} - P_t^f \delta_t^f + \tilde{P}^{el} \tilde{\delta}_t^{el} + \tilde{P}^f \tilde{\delta}_t^f, \quad (2)$$

$$P_{min}^f \delta_t^f \leq P_t^f \leq P_{max}^f \delta_t^f, \quad (3)$$

$$P_{min}^{el} \delta_t^{el} \leq P_t^{el} \leq P_{max}^{el} \delta_t^{el}, \quad (4)$$

$$\delta_t^{el} + \delta_t^f + \tilde{\delta}_t^{el} + \tilde{\delta}_t^f = 1, \quad (5)$$

$$H_{t+1} = H_t + \frac{\Delta}{E^h} (\phi_t^{el} - \phi_t^f), \quad (6)$$

$$H_{min} \leq H_t \leq H_{max}, \quad (7)$$

where: P_t^r is the power exchanged by the RFC, positive when absorbing, negative when generating; P_{max}^{el} , P_{min}^{el} , P_{max}^f and P_{min}^f are, in the following order, maximum and minimum power of SOEC and SOFC; H_t [p.u.] is the Hydrogen Level in the Tank (SoH); H_{min} and H_{max} are minimum and maximum SoHs; E^h [Wh] is the tank capacity, defined according to the transformation $1 \text{ MW h} = 30 \text{ kg}$; ϕ_t^{el} and ϕ_t^f are the power exchanged by the RFC with the tank, respectively in SOEC and SOFC mode. ϕ_t^{el} and ϕ_t^f are nonlinear functions of P_t^{el} and P_t^f , respectively.

δ_t^{el} , δ_t^f , $\tilde{\delta}_t^{el}$ and $\tilde{\delta}_t^f$ are binary variables representing the operating mode of the RFC, respectively: SOEC mode, SOFC mode, transition to Solid-Oxide Electrolyzer Cell (t-SOEC) mode and transition to Solid-Oxide Fuel Cell (t-SOFC) mode. In order to switch from SOEC to SOFC, the RFC has to operate in t-SOFC mode before operating in SOFC mode, similarly in order to switch from SOFC to SOEC, the RFC has to operate in t-SOEC mode first. Furthermore, when t-SOFC or in t-SOEC mode occurs, the RFC must operate as a SOFC or as a SOEC, respectively, in the following time interval. Finally in order to curtail mechanical and thermal stress, the number of switches between the operating modes should be limited. All of these conditions are modeled with the following mixed integer constraints:

$$\delta_t^{el} + \delta_{t+1}^f \leq 1, \quad \delta_t^{el} + \tilde{\delta}_{t+1}^{el} \leq 1, \quad (8)$$

$$\delta_t^f + \delta_{t+1}^{el} \leq 1, \quad \delta_t^f + \tilde{\delta}_{t+1}^f \leq 1, \quad (9)$$

$$\tilde{\delta}_t^{el} - \delta_{t+1}^{el} \leq 0, \quad \tilde{\delta}_t^f - \delta_{t+1}^f \leq 0, \quad (10)$$

$$\sum_{j=0}^M (\tilde{\delta}_{t+j}^{el}) \leq \alpha, \quad \sum_{j=0}^M (\tilde{\delta}_{t+j}^f) \leq \alpha. \quad (11)$$

Constraint (11) is introduced to limit mechanical and thermal stress; α is the maximum number of switches allowed in M time-steps from the current time t .

C. REC

According to Italian transposition of REM and RED II [12], a REC is paid for the energy self-consumed between the members of the community and for the energy sold to

the grid. The self-consumed energy $\Delta \cdot P_t^{ac}$ is defined as the minimum between the energy exported by the manager and the one consumed by the members of the REC:

$$P_t^{ac} = \min(P_t^e, P_t^l) \quad (12)$$

where P_t^l is the power demand at time t of the warehouses aggregate.

Since according to the manager economic return (17), introduced below, both P_t^{ac} and P_t^e will be maximized, (12) can be rewritten by the following inequalities:

$$P_t^{ac} \geq 0, \quad (13)$$

$$P_t^{ac} \leq P_t^e, \quad (14)$$

$$P_t^{ac} \leq P_t^l. \quad (15)$$

D. Power Balance, Operational Costs and Available Data

During every quarter hour t , the following power balance has to be matched:

$$P_t^{res} = P_t^r + P_t^e, \quad (16)$$

and the manager economic return is:

$$J_t = \Delta((c^m + c^r)P_t^{ac} + c_t^e P_t^e) \quad (17)$$

where P_t^{res} is the power generated by RES; c_t^e is the energy sell-back price; c^m is an incentive bestowed by the Italian Ministry of Economic Development (MISE) and c^r is the restitution of grid charges since P_t^{ac} does not burden on the grid [12]. The objective of the paper is to maximize the REC manager economic return, assuming that at time step t , given a time horizon T , the following data are available:

- a set of S scenarios each one containing a forecast profile of RES generation $\{\hat{P}_{t+k}^{res}(s)\}_{k=0}^{T-t-1}$, a forecast profile of load $\{\hat{P}_{t+k}^l(s)\}_{k=0}^{T-t-1}$, and an associated confidence probability $\pi_t(s)$ associated at the mentioned scenario $s = 1 \dots S$;
- the current SoH H_t ;
- all energy prices from time t to time $t + T - 1$.

III. OPTIMAL MANAGEMENT

In this section we propose the optimal management algorithm, which decides a control action at each time-step t , given the data above reported. At quarter hour t , we will indicate with $k = 0, 1, \dots, T - 1$ the time sequence $t, t + 1, \dots, t + T - 1$.

In the following, we first introduce the method adopted to obtain load and RES forecasts, and then we formulate a Mixed Integer Linear Problem (MILP), finally used by an MPC controller to perform the optimal management.

A. Load and RES Generation Forecasts

In [5], a methodology named Instantaneous Growing Stream Clustering (IGSC) has been proposed to model time series of interest with a DMC through an adaptive online algorithm with minimal computational efforts. The constructed DMC can then be used to sample possible future scenarios (forecasts) given the current actual state of the DMC.

The states dwell in the same space of the measurements (e.g. in the active power-time plane) and are characterized by the mean of the measurements that happened to be closest to that state. For each state also the number of measurements, their variance, and covariance between the variables are kept in memory.

The algorithm presents just one parameter: τ , a positive real number, which regulates how different from current states must be a new measurement in order to add a new state to the DMC (the optimal choice of τ has been investigated in [13]). The algorithm is detailed in the following for the case of two variables.

Let $m(x) = [m_1(x), m_2(x)]$ the mean vector of a state x , $\sigma(x) = [\sigma_1(x), \sigma_2(x)]$ the variances of a state x , $\rho(x)$ the covariance of a state x and $N(x)$ the measurement assigned to a state x . Let $O_k = [O_{1,k}, O_{2,k}]$ be the current observation and x_{k-1} the last timestep state. The steps of the proposed algorithm for each incoming measurement are the following:

- 1) Matching step: Find the two states closest to O_k , respectively F_k and S_k ;
- 2) State Adaptation: create a new state with the same coordinates of O_k , connect it with F_k and assign it to x_k (current state) if:
 - O_k is outside the circle of diameter $\overline{F_k S_k}$;
 - The Euclidean distance between O_k and F_k is greater than τ ;
otherwise do not create a new state, instead let $x_k = F_k$
- 3) Weight adaptation: The state x_k , to which O_k has been assigned, is updated. For each variable $i = 1, 2$, the mean is updated as follows:

$$m_i(x_k) := \frac{m_i(x_k) \cdot N(x_k) + O_k}{N(x_k) + 1} \quad (18)$$

With similar formulas the variance of each variable and the covariance between each pair of variables are updated for current state x_k :

$$\sigma_i(x_k) := \frac{\sigma_i(x_k) \cdot N(x_k) + (O_k - m_i(x_k))^2}{N(x_k) + 1} \quad (19)$$

$$\rho(x_k) := \frac{1}{N(x_k) + 1} \cdot \rho(x_k) \cdot N(x_k) + \frac{1}{N(x_k) + 1} (O_{1,k} - m_1(x_k)) \cdot (O_{2,k} - m_2(x_k)) \quad (20)$$

Finally, $N(x_k)$ is increased by one.

- 4) Edge Adaptation: A link between the past state x_{k-1} and the current state x_k is created, if it does not exist. Moreover, the weights of all the links starting from the past state are changed to reflect the transition probability.

The resulting DMC is used for the simulation of possible future scenarios, given the current state and using the transition probabilities between the states.

In order to add some variability, the simulated values are not exactly equal to the mean of the states, but they are added to a realization of a bivariate normal random variable having

as covariance matrix the variance and covariances computed for each state during the weight adaptation steps.

To be used by the control algorithm, the DMC is first trained on historical data. Then, at time t , given the actual values of RES generation P_t^{res} and power demand P_t^l , a set of 300 paths of length $T + 1$ is generated. The set is then reduced to 10 scenarios with same length and a probability $\pi_t(s)$ is associated to each of them, applying the scenario reduction method introduced in [14].

B. Piecewise linearization of nonlinearities

Equation (6), for any $t = k$, is nonlinear, since ϕ_k^{el} and ϕ_k^{ef} are nonlinear functions of P_k^{el} and P_k^f , i.e. $\phi_k^{el} = g^{el}(P_k^{el})$ and $\phi_k^{ef} = g^f(P_k^{el})$. To cope with this, Special Ordered Set of type 2 (SOS2) variables are introduced. SOS2 is an ordered set of non-negative variables, of which at most two of them can be non-zero and if two are non-zero they must be contiguous in the ordered set. Given the set $\Lambda = \{\lambda^l\}_{l=1}^L$ of length L it has to be:

$$\sum_{l=1}^L \lambda^l = 1, \quad \lambda^l \geq 0 \quad (21)$$

$$\text{if } \lambda^{l'} > 0 : \begin{cases} \lambda^{\bar{l}} = 0 \\ \lambda^{l'+1} \geq 0 \end{cases} \quad \bar{l} \in [1, L] \wedge \bar{l} \neq l, l+1 \quad (22)$$

$l' \in [1, L-1]$

SOS2 variables are adopted to approximate functions $g^{el}(\cdot)$ and $g^f(\cdot)$, as it follows:

$$P_k^\mu = \sum_{l=1}^L \lambda_k^l P^{\mu,l}, \quad \phi_k^\mu = \sum_{l=1}^L \lambda_k^l \phi^{\mu,l} \quad (23)$$

where $\mu = el, f$, $P^{\mu,l}$ are the independent variable breakpoints, $\phi^{\mu,l}$ are the value of functions at the breakpoints (intercepts: $\phi^{\mu,l} = g^\mu(P^{\mu,l})$), and λ_k^l are the SOS2 variables.

C. Two-stage Stochastic Optimization Problem

In a two-stage stochastic programming approach the sum of two cost functions is minimized, the first-stage one refers to the actual objective of the optimization, the second-stage one is suitably defined to minimize the expected violation of constraints that involve random variables. Specifically, such uncertain constraints are relaxed by introducing positive auxiliary variables, called *recourse variables*. The value of these variables is then minimized according to second-stage cost function, that is suitably defined to take into account the probability distributions of the random variables. For details, the reader is referred to [6], [7].

According to (17), first-stage cost function is:

$$J^{fs} = - \sum_{k=0}^{T-1} \Delta ((c^m + c^r) P_k^{ac} + c_k^e P_k^e) \quad (24)$$

and constraints are (1)–(11), (15)–(16), (23). Constraints that involve random variables are (15) and (16). Therefore, first we

rewrite (15) as equality constraint, $\forall k \in [0, T-1]$:

$$P_k^{ac} + \gamma_k = P_k^l, \quad \gamma_k \geq 0, \quad (25)$$

where γ_k are slack positive variables; then, we rewrite (25) and (16), as second-stage constraints: $\forall k \in [0, T-1]$ and $\forall s \in [1, S]$,

$$\xi_k^+(s) \geq P_k^{ac} + \gamma_k - \hat{P}_k^l(s), \quad (26)$$

$$\xi_k^+(s) \geq 0, \quad (27)$$

$$\xi_k^-(s) \geq \hat{P}_k^l(s) - P_k^{ac} - \gamma_k, \quad (28)$$

$$\xi_k^-(s) \geq 0, \quad (29)$$

$$\gamma_k \geq 0, \quad (30)$$

$$\chi_k^+(s) \geq P_k^r + P_k^e - \hat{P}_k^{res}(s), \quad (31)$$

$$\chi_k^+(s) \geq 0, \quad (32)$$

$$\chi_k^-(s) \geq \hat{P}_k^{res}(s) - P_k^r - P_k^e, \quad (33)$$

$$\chi_k^-(s) \geq 0. \quad (34)$$

where $\chi_k^+(s)$, $\chi_k^-(s)$, $\xi_k^+(s)$ and $\xi_k^-(s)$ are the recourse variables; finally, the second-stage cost function is defined as follows:

$$J_t^{ss} = \sum_{k=0}^{T-1} \sum_{s=1}^S \pi_t(s) [(\chi_k^+(s) + \xi_k^+(s)) \omega^+ + (\chi_k^-(s) + \xi_k^-(s)) \omega^-], \quad (35)$$

where ω^+ and ω^- are penalty weights. In (35) we can observe how, using the probability distribution $\pi_t(s)$ of scenarios, recursive variables are minimized as higher is the probability that the corresponding scenarios occur.

To conclude, the two-stage stochastic optimization problem is formulated by the following MILP:

$$\min_{\{X_k\}_{k=0}^{T-1}} (J_t^{fs} + J_t^{ss}) \quad (36)$$

$$X_k = [P_k^e, P_k^{el}, P_k^f, \delta_k^{el}, \delta_k^f, \tilde{\delta}_k^{el}, \tilde{\delta}_k^f]^\top$$

subject to: (1)–(11), (14), (23), (26)–(34).

D. Control Algorithm

The algorithm consists in solving (36) at each time-step t . Then, the *receding horizon* is adopted: to apply just the values calculated for the instant $k = 0$ to the controlled variable, move to the successive time-step $t + 1$, and repeat the same procedure. Forecasting errors are compensated outside the optimization problem with the aim of maximizing the income of the REC manager. Therefore, if the actual RES generation is higher than the expected one, P_t^e is increased to exploit the surplus in generation and increase the income; instead, if it is lower, P_t^r is increased, when possible according to (1)–(7), otherwise P_t^e is decreased. Changes in P_t^r and P_t^e are made to keep always satisfied (16).

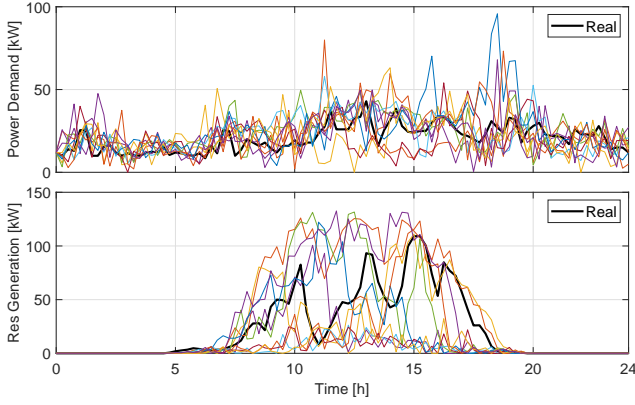


Figure 2. Example of 10 scenarios generated at midnight of the third day of simulations for warehouses aggregated demand (top) and RES generation (bottom).

IV. CASE STUDY

The considered case study is an aggregation of industrial warehouses equipped with PV generators. The industrial aggregation is supposed to undergo Italian regulation [12]. Data of power demand and PV generation are taken from [15]. In particular, power demand was taken as it was, while PV generation was increased in nominal power with respect to the values reported in [15]. Values of nominal power demand and nominal PV generation are listed in Table I.

To get forecasts, the method described in Section III-A is applied with $\tau = 0.1$. The DMC is trained with historical data in [15]. Figure 2 shows an example of 10 scenarios generated for RES production and power demand at the midnight of the third day of simulation in comparison with their real values.

The developed model correlates the power, in terms of hydrogen production (SOEC) or consumption (SOFC), with the number N_c of SOCs constituting the RFC, the operating temperature θ of the SOCs, and the electrical powers used P^{el} and produced P^f . The investigated relations are:

$$\eta^{el} = \frac{N_{H_2}^{el} LHV_{H_2}}{P^{el}} = \frac{\phi^{el}}{P^{el}}, \quad (37)$$

$$\eta^f = \frac{P^f}{N_{H_2}^f LHV_{H_2}} = \frac{P^f}{\phi^f}, \quad (38)$$

where η^{el} and η^f are efficiencies in SOEC and SOFC mode, $N_{H_2}^{el}$ and $N_{H_2}^f$ the flow of hydrogen produced in SOEC mode and consumed in SOFC mode, LHV_{H_2} the Lower Heating Value of hydrogen, P^{el} the power that has to be given in SOEC mode to produce $N_{H_2}^{el}$ ensuring isothermic operation, warming up the reagents and compressing the produced hydrogen, finally P^f the electric power produced by the SOFC deduced by the power to warm up the reagents. SOC working conditions are fixed in order to optimise the operation basing on authors' previous work [16].

In the following equations we provide the numerical expres-

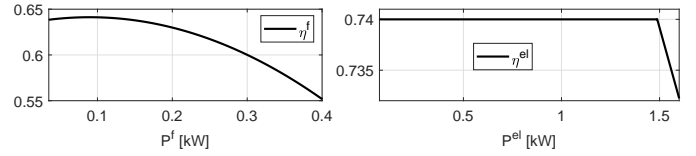


Figure 3. Single cell efficiencies in SOFC (left) and SOEC (right) modes, with $\theta = 1123$ K.

Table I
STUDY CASE PARAMETERS

| Parameter | Symbol | Value |
|------------------------------------|------------------|-------------|
| Main Grid Connection Nominal Power | P_{max}^g | 340 kW |
| Storage Capacity | E^h | 400 kW h |
| RFC Number of SOCs | N_c | 100 |
| Minimum Power in SOEC mode | P_{min}^{el} | 7.2 kW |
| Maximum Power in SOEC mode | P_{max}^{el} | 160 kW |
| Minimum Power in SOFC mode | P_{min}^f | 3.5 kW |
| Maximum Power in SOFC mode | P_{max}^f | 40 kW |
| RFC Power Demand in t-SOEC mode | \tilde{P}^{el} | 2.6 kW |
| RFC Power Demand in t-SOFC mode | \tilde{P}^f | 1.3 kW |
| Nominal Power Demand | — | 163 kW |
| PV Plant Nominal Power | — | 150 kW |
| MISE Incentive | c^m | 0.11 €/kWh |
| Restitution of Grid Charges | c^r | 0.009 €/kWh |

sions of η^{el} and η^f .

$$\eta^{el} = \begin{cases} 0.74 & \frac{P^{el}}{N_c} \leq (\alpha_1 \theta^2 - \alpha_2 \theta + \alpha_3) \\ \beta_1 \frac{\theta P^{el}}{N_c} - \beta_2 \frac{P^{el}}{N_c} + \beta_3 \theta & \frac{P^{el}}{N_c} > (\alpha_1 \theta^2 - \alpha_2 \theta + \alpha_3) \end{cases} \quad (39)$$

$$\eta^f = 8.06 \times 10^{-3} \frac{\theta P^f}{N_c} - 8.89 \frac{P^f}{N_c} + 1.85 \times 10^{-2} \theta - 9.29 \times 10^{-1} \left(\frac{P^f}{N_c} \right)^2 - 8.95 \times 10^{-6} \theta^2 - 8.88 \quad (40)$$

where $\alpha_1 = 4.87 \times 10^{-4}$, $\alpha_2 = 9.46 \times 10^{-2}$, $\alpha_3 = 46.34$, $\beta_1 = 2.32 \times 10^{-4}$, $\beta_2 = 0.33$ and $\beta_3 = 7.7 \times 10^{-4}$. The profiles of the two efficiencies, for the constant operating temperature $\theta = 1123$ K are shown in Figure 3.

From (37)–(39) and (40), it is possible to express functions $\phi^{el} = g^{el}(P^{el})$ and $\phi^f = g^f(P^f)$, then used by the control algorithm as described in Section III-B.

The number of SOCs composing the RFC was estimated by setting the upper power in SOEC mode equal to the maximum value of power demand. The maximum number of switches between operating modes is set to 3 in 4 h.

V. SIMULATION RESULTS

To test the performance of the proposed control algorithm, one week has been simulated, using the data from the midnight of June 4th to the midnight of June 12th, 2017. The values adopted for c^c , c^m and c^r are listed in Table I, c_t^e is shown in Figure 4 and it represents to the actual energy clearing market price in Italy. Notice that the energy prices considered in this application are the characteristic values at the beginning of 2021, before the sudden rise of natural gas price in Europe.

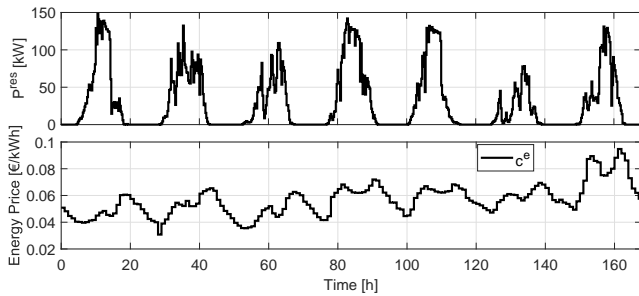


Figure 4. RES generation (top) and energy price (bottom) profiles.

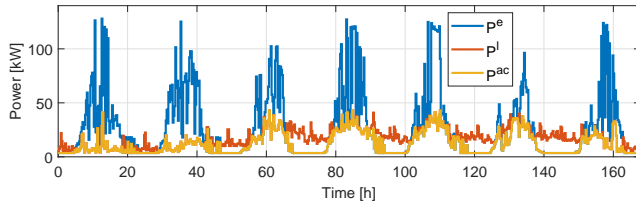


Figure 5. REC power profiles.

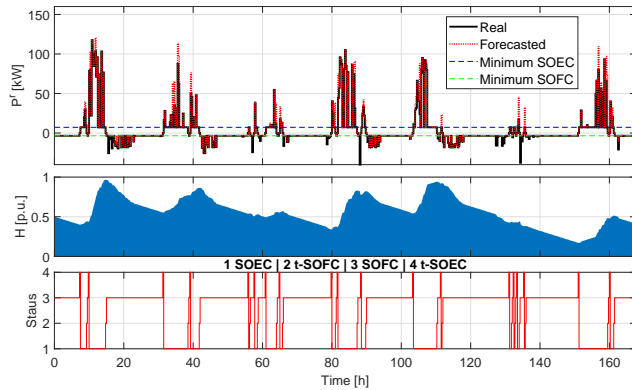


Figure 6. RFC exchanged power (top), SoH (mid) and operating mode (bottom).

The following control parameters have been set as: $T = 24$ h, $S = 10$ scenarios, $H_{max} = 1$ p.u. and $H_{min} = 0$ p.u. The values of penalty weights ω^+ and ω^- were set to 1, about ten times higher than the values of the other prices.

The control algorithm has been implemented in MATLAB, integrated with General Algebraic Modeling System (GAMS) to write the optimization problem, solved by CPLEX solver.

Figures 5–6 show an example of obtainable simulation results. In particular in Figure 6 we can observe how the RFC is managed: during the nights, the algorithm decides to discharge the hydrogen tank and to never switch between two modes since any transition represents an additional load that can not be satisfied in absence of RES generation. Furthermore we can observe that the majority of switches is obtained during the days with less RES generation.

We finally remark that the total earning obtained within the week operations has resulted to be equal to 2044.45€, against 1955.58€ obtained in the same conditions without the RFC.

VI. CONCLUSIONS

In this paper a control strategy for a RFC used to manage a REC is proposed. A two-stage scenario-based MPC algorithm has been designed to decide the best economic strategy to be followed during operations. Such an algorithm uses a suitably defined DMC based method to forecast consumers demand and renewable generation, and a nonlinear model of RFC efficiency derived from a physical based model at local level. The algorithm has been successfully tested on a REC composed by an aggregation of industrial buildings and a PV plant.

REFERENCES

- [1] “Empowering Variable Renewables: Options for Flexible Electricity Systems,” IEA, Tech. Rep., 2008.
- [2] F. Conte, F. D’Agostino, P. Pongiglione, M. Saviozzi, and F. Silvestro, “Mixed-integer algorithm for optimal dispatch of integrated pv-storage systems,” *IEEE Trans. Ind. Appl.*, vol. 55, no. 1, pp. 238–247, 2019.
- [3] A. Gallo, J. Simoes-Moreira, H. Costa, M. Santos, and E. Moutinho dos Santos, “Energy storage in the energy transition context: A technology review,” *Renewable and Sustainable Energy Reviews*, vol. 65, pp. 800–822, Jul. 2016.
- [4] G. L. Soloveichik, “Regenerative fuel cells for energy storage,” *Proceedings of the IEEE*, vol. 102, no. 6, pp. 964–975, 2014.
- [5] S. Massucco, G. Mosaico, M. Saviozzi, F. Silvestro, A. Fidigatti, and E. Ragaini, “An instantaneous growing stream clustering algorithm for probabilistic load modeling/profiling,” in *2020 Int. Conf. on Probabilistic Methods Applied to Power Systems (PMAPS)*, 2020, pp. 1–6.
- [6] A. Parisio and C. Neil Jones, “A two-stage stochastic programming approach to employee scheduling in retail outlets with uncertain demand,” *Omega*, vol. 53, no. C, pp. 97–103, 2015.
- [7] A. Parisio, E. Rikos, and L. Glielmo, “Stochastic model predictive control for economic/environmental operation management of microgrids: an experimental case study,” *J. Proc. Control*, vol. 43, pp. 24–37, 2016.
- [8] Z. Zhang, Y. Nagasaki, D. Miyagi, M. Tsuda, T. Komagome, K. Tsukada, T. Hamajima, H. Ayakawa, Y. Ishii, and D. Yonekura, “Stored energy control for long-term continuous operation of an electric and hydrogen hybrid energy storage system for emergency power supply and solar power fluctuation compensation,” *International Journal of Hydrogen Energy*, vol. 44, pp. 8403–8414, 2019.
- [9] L. Mastropasqua, I. Pecinati, A. Giotri, and S. Campanari, “Solar hydrogen production: Techno-economic analysis of a parabolic dish-supported high-temperature electrolysis system,” *Applied Energy*, vol. 261, p. 114392, 2020.
- [10] European Commission, “Directive on common rules for the internal electricity market ((eu) 2019/944),” 2019.
- [11] —, “Revised renewable energy directive (2018/2001/eu),” 2018.
- [12] Italian Council of Ministers, “Decreto legislativo 8 novembre 2021, n. 199 attuazione della direttiva (ue) 2018/2001 del parlamento europeo e del consiglio, dell’11 dicembre 2018, sulla promozione dell’uso dell’energia da fonti rinnovabili,” [In Italian].
- [13] S. Massucco, G. Mosaico, M. Saviozzi, F. Silvestro, A. Fidigatti, and E. Ragaini, “A markov chain load modeling approach through a stream clustering algorithm,” in *2020 AEIT Int. Annual Conf.*, 2020, pp. 1–6.
- [14] N. Growe-Kuska, H. Heitsch, and W. Romisch, “Scenario reduction and scenario tree construction for power management problems,” in *IEEE PowerTech*, vol. 3, Bologna, Italy, 2003, pp. 1–7.
- [15] <https://data.open-power-system-data.org/householddata/2020-04-15>.
- [16] F. Bianchi and B. Bosio, “Operating Principles, Performance and Technology Readiness Level of Reversible Solid Oxide Cells,” *Sustainability*, vol. 13, p. 4777, 2021.